Cactus Stem Inspired Cone-Arrayed Surfaces for Efficient Fog Collection

*Jie Ju, Xi Yao, Shuai Yang, Lin Wang, Ruize Sun, Yaxu He, and Lei Jiang**

With the increasing world population and the rapid development of the global industry, clean water is becoming scarcer and scarcer. Means of translating latent water in fog to dominant available water, i.e., fog collection, therefore becomes highly desirable. Previously, it was demonstrated that the cactus *O. Microdasys* has an integrated fog collection system arising from the evenly distributed clusters of spines and trichomes on the cactus stem. Here, it is reported that the intersite of the clusters on the cactus stem is densely covered with cones, which are also capable of collecting water from fog efficiently. Inspired by these cones, using a simple method combining mechanical perforating and template replica technology, polydimethylsiloxane (PDMS) cone arrays are fabricated with different arrangements and the one in hexagonal arrangement proves to be more efficient due to the more turbulent flow filed around the staggered cones and the rapid directional movement of water drops along each cone. This investigation opens up new avenue to collect water efficiently and may also provide clues to research about dust filtering and smog removal, which is attracting increasing attention worldwide.

1. Introduction

Water is of vital importance to living organisms. Unfortunately, in many parts of the world, such as most of Africa and parts of South America, the access to adequate water from precipitation is always no way.[1] To survive in these regions, many plants and animals have evolved special surface structures facilitating the collection of water from the frequent occurrence of dense fog.[2] For instance, the famous Namibia Desert beetles utilize their backs, which have hydrophobic and hydrophilic patterns, to collect water from fog;[3] a kind of Namibia dune grasses can also intercept tiny water drops contained in fog and transport them along their ridged and grooved leaves to roots, thus realizing self-irrigation.[4] Taking inspiration from these creatures, many fog collectors based on alternative surface wettability[5] and structured fibers[6] have been developed. However, all of these fog collectors share common drawbacks: the tiny water drops collected on them are unable to perform directional movement and the deposition sites on the fog collectors can not be released in time. This delayed surface refreshment further counts against efficient fog collection.[7] Most recently, a cactus (*O. Microdasys*) was discovered to be able to collect water continuously and efficiently by making using of its clusters of conical spines and belt-structured trichomes on the succulent stems.[8] Due to the conical structures, microsized water drops collected can be transported directionally away from the original deposition site under the gradient of Laplace pressure as soon as they grow to a critical size, just as the directional movement of tiny water drops on natural and artificial spider silks.[9,10] This quick regeneration of the deposition sites guarantees rapid begin of next cycle of "fog deposition – drop directional movement – water collection", facilitating the efficient fog collection.

In addition to the clusters of spines and trichomes, we find that the intersite of the clusters on cactus stem is covered with densely distributed cones, contributing to the overall fog collection. Inspired by these cones, using a simple method combining mechanical perforating and template replica technology, we fabricate polydimethylsiloxane (PDMS) cone arrays with different arrangements and the one in hexagonal arrangement proves more efficient due to the more turbulent flow filed around the staggered cones and the rapid directional movement of water drops on each cone.

Dr. J. Ju, Dr. X. Yao, Prof. L. Jiang
Beijing National Laboratory
for Molecular Science (BNLMS)
Institute of Chemistry
Chinese Academy of Sciences
Beijing, 100190, P. R. China
E-mail: jianglei@iccas.ac.cn
Dr. S. Yang, Mr. L. Wang, Dr. R. Sun, Ms. Y. He
School of Chemistry and Environment
Beihang University
Beijing, 100191, P. R. China
Dr. J. Ju
Graduate University of Chinese Academy of Sciences
Beijing, 100049, P. R. China

DOI: 10.1002/adfm.201402229

2. Results and Discussion

2.1. Microstructures and Fog Collection Ability of Natural Cactus Stem

As shown in **Figure 1**A, there are many clusters of spines on the cactus stem, among which the densely distributed cones can be observed. These cones have an apex angle of about 22.67° ± 5.29°, height of about 105.96 ± 28.37 μm, distance

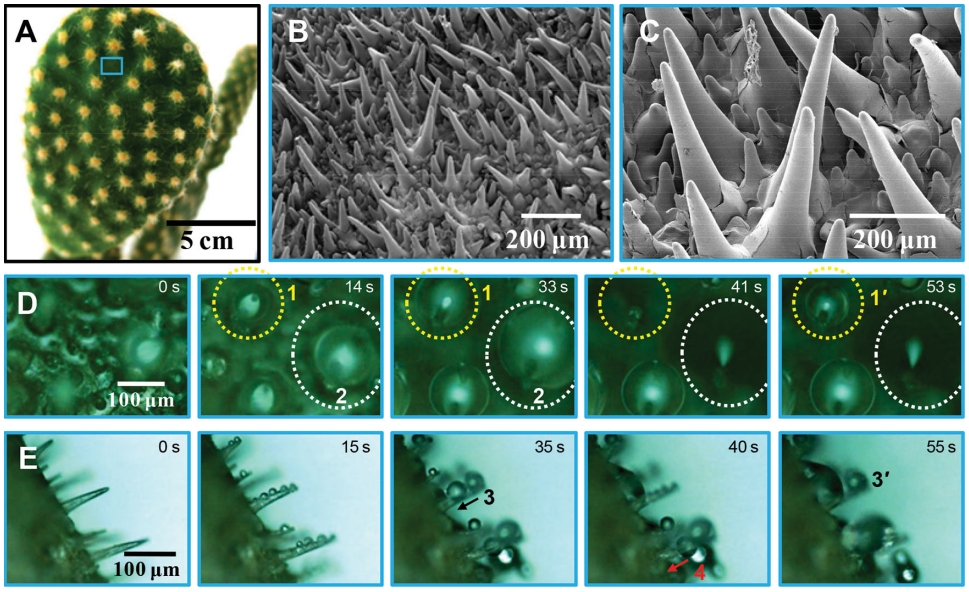

Figure 1. Appearance and fine structures of cactus stem and its fog collection performance. A) Stem of cactus *O. Microdasys* covered with clusters of spines and densely distributed microsized cones. B,C) Scanning electron microscopy (SEM) images of the microsized cones, showing a relatively smooth surface. D) Top-view and E) side-view of the cactus stem in fog flow at room temperature. Tiny water drops deposited on the cones (drop 1, 2, 3 and drop 4) move from tip towards base of the cones and new drops (drop 1′, drop 3′) appear again on the freshly released tip region

between adjacent cones in the tip about 89.62 ± 28.06 µm, and the surface of them are relatively smooth (Figure 1B,C). Static water contact angle measurement of the stem surface gives a value of about 147.4°, showing superhydrophobicity (Supporting Information Figure S1). Removing the clusters of spines on the cactus stem and placing the stem with a tilted angle θ to the horizontal surface, meanwhile, keeping a sustained fog flow with a velocity of about 125 cm s^{-1} blowing to the surface with a tilted angle δ to the tangent direction of the cone-structured surface at room temperature (see Experimental Section and Supporting Information Scheme S1). As the deposition precedes, tiny water drops deposited on the cones, such as drop 1 and drop 2 depicted with yellow and white circles in the top-view images and drop 3 in the side-view images, move directionally towards the base of the cones with larger curvature radii due to the gradient of the Laplace pressure.[11,12] The original deposition sites are thus released, ready for next cycle of fog collection, which can be verified by the newly appeared drops 1′, 2′ and 3′ at the same location as drops 1, 2 and drop 3. This continuous and directional transport of microsized water drops is beneficial for the efficient fog collection.

2.2. Fabrication and Characterization of Cactus Stem Inspired Cone Arrays with Different Arrangements

2.2.1. Fabrication and Structures of Artificial Cone Arrays

Inspired by the principle of multiple cones' collective fog collection, we prepared the artificial cone arrays in different arrangements using a simple method combining mechanical perforating and template replica technology,[13] see Supporting Information Figure S2 and Experimental Section. **Figure 2**A–C and Figure 2D-F are SEM images of the as prepared PDMS cone arrays in hexagonal and tetragonal arrangement, respectively. In both arrangements, these cones share the similar dimension parameters: height of the cones of about 634.1 ± 6.7 µm, diameter of the cones at the base of about 119.2 ± 4.3 µm and the distance between the adjacent cones at the tip of about 368.3 ± 17.7 µm. Closer observation of the cones shows that the surfaces of these microsized cones are sculptured with longitudinal nanogrooves (Supporting Information Figure S3), similar to the ridged surface of the desert dune grass's leaf, which may be helpful in directing water drops collected to the base of the cones.[4]

2.2.2. Fog Collection Ability of Artificial Cone Arrays

To test the water collection ability of these cone-structured surfaces, we first put the surface with hexagonally arranged cones into the same fog flow as before (Supporting Information Scheme S1). From the 45° Tiled-view in **Figure 3**A and the Side-View in Figure 3B, we can see that tiny water drops initially deposit randomly on the PDMS cone surfaces (a_2 and b_2). As the deposition continuous, water drops move towards base of the cones with their size increasing (a_3-a_4, b_3-b_5), meanwhile, refreshing the origional deposition sites. As soon as the newborn surface forms, another tiny water drop (1′ and 2′) appears at the same location of the former drop (a_5, b_4). The next cycle of "fog deposition – drop directional movement – water collection" begins. The following experiments of water collection on the surface with tetragonally arranged cones behave similarly, experiencing the same fog deposition, directional drop movement and incessant fog collection (Supporting Information Figure S4). Notably, there are two modes in water drops'

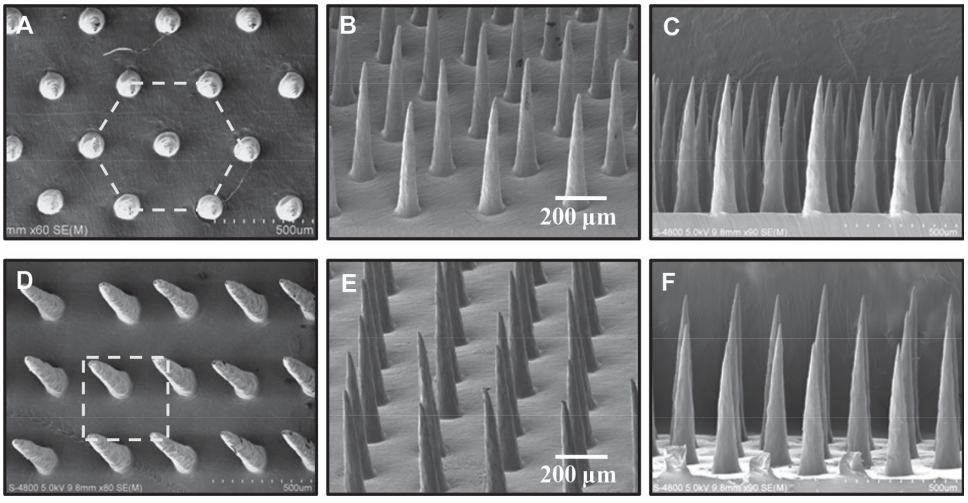

Figure 2. SEM images of the cactus stem inspired PDMS cone arrays in different arrangements. A–C) Hexagonally arranged PDMS cone arrays. D–F) Tetragonally arranged PDMS cone arrays. A,D) Top-view, B,E) 45° tiled-view, and C,F) side-view. The height of the PDMS cones, diameter of the cones at base, and distance between the cones at tips are all similar in both arrangements and are approximately 634.1 ± 6.7 μm, 119.2 ± 4.3 μm and 368.3 ± 17.7 μm, respectively.

directional movement with the same gradient of Laplace pressure: water drops on the surface of cones can move directly towards base of the cones as their size is large enough to overcome the resistence from contact angle hysteresis,[14] such as drop 1, drop 2 in Figure 3B, or they may merge with adjacent drops first and then move directionally, similar to drop 1+2, drop 3+4 shown in Supporting Information Figure S4. The latter case is believed to be more favourable for driving water

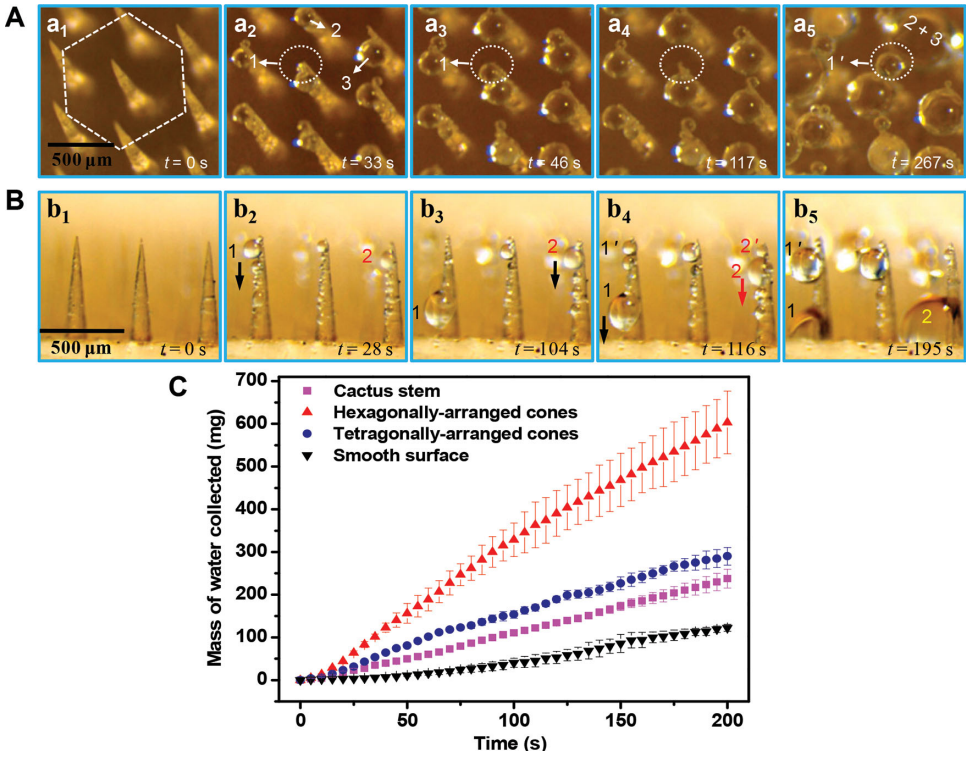

Figure 3. Optical observation of the fog collection behavior of hexagonally arranged cone array in A) 45° tilted-view and B) side-view. Water drops deposited randomly on the cones move directly towards base of the cone (drop 1 in (A) and drop 1, 2 in (B)) or merge with adjacent drops first and then move towards base of the cone (drop 2+3 in (A)), refreshing the original sites for the next cycle of deposition, as indicated by the new appearing drop 1′ and drop 2′. C) Statistical comparison of mass of the water collected on four types of surfaces along the deposition time under the same fog condition. At a fixed time, the surface with hexagonally arranged cones shows larger fog collection efficiency than the natural cactus stem and collects the most water, while the smooth surface collects the least water.

drop to move due to the energy feed upon drops coalescence, which helps to overcome the energy barrier arising from contact angle hysteresis against drop movement.[15] Because the dimension parameters in both structured surfaces are the same, the mode of movement that the drop adopts is therefore largely random. Additionally, the inclined placement of the cone-structured surface is vital to drain the water collected. When the water drops collected get to the bottom of the cones, they merge with each other. The forming large drops slip down to the container below and the fog collector surface refreshes. In addition to the gravitation force-assisted drain method we used here, peristaltic pump with rubber tube connected to the bottom of the fog collector surface[16] or hydrophilic absorption materials fixed at the substrate[17] have also been developed to transfer the water collected.

In addition to the cone-structured surface, we also investigated the fog collection performance of smooth PDMS with a thickness equaling to the overall thickness of PDMS substrate plus height of PDMS cones of cone-structured surfaces (Supporting Information Scheme S1). Supporting Information Figure S5 shows the microscale flatness of the smooth PDMS. The experimental installation is the same as that in fog collection experiments of cone-structured surfaces. Under the fog condition, tiny water drops randomly deposite on the smooth PDMS surface. With continued deposition, the water drops increase their size through directly capturing microsized drops in fog or coalescsing with other drops nearby but without obvious transfer of mass center in either case (Supporting Information Figure S6). This abscence of quick regeneration of the fresh deposition sites in the overall process counts against the inventual fog collection.

To quantitatively display the superity of the cone-structured surfaces in collecting fog efficiently, four kinds of surfaces, including the natural cactus stem, surface with hexagonally arranged PDMS cones, surface with tetragonally arranged PDMS cones and smooth PDMS surface with the same dimension (1 cm by 1 cm) were placed in the same fog flow and their mass change along the depositon time is plotted in one table. As can be seen from Figure 3C, in a time range from 0 s to 200 s, surface with hexagonally arranged cones collects the most water, while smooth PDMS collect the least. In detail, mass of the water collected on the surface with hexagonally arranged cones, surface with tetragonally arranged cones and natural cactus stem is, repectively, about 4.9 times, 2.4 times and 1.9 times of that on the smooth surface after 200 s. In other words, for the three kinds of artificial surfaces, the fog collection efficiency decreases from surface with hexagonally arranged cones to surface with tetragonally arranged cones to the smooth surface. Moreover, when a polypropylene mesh (with shading coefficient of about 62.37% and size of 1 cm × 1 cm) widely used in fog collection project was placed in the same fog condition and keep the fog flow blowing perpendicularly to the surface of the mesh, its water collection efficiency is also smaller than the surface with hexagonally arranged cones but larger than other cone-structured surfaces and the smooth surface within 200 s, as shown in Supporting Information Figure S7. These quantitative comparison clearly shows that surface with hexagonally arranged cones are the most efficient in collecting fog.

2.3. Mechanism for the Different Fog Collection Ability

Considering the artificial cone-structured surfaces and the smooth surface, since the fog condition imposed for them and their chemical composition, PDMS, are all the same, the efficiency discrepancies may mainly arise from the consequences owing to different structures: different fog flow fields and directional movement of water drops on cone-structured and smooth surfaces.

2.3.1. Distinct Fog Flow Field Around Different Structured Surfaces

Fog collection occurs when tiny water drops with diameter ranging from 8–40 μm contained in a fog flow are intercepted by the obstacle forward.[18] Ideally, the tiny water drops will advance with the fog flow. In view of the fog flow, when it gets close to the obstacle, the part that falls to the boundary of the obstacle's projection plane is inevitablly deflected due to the resistance force and continues to flow downstream. Tiny water drops contained in this part of flow advances with the flow waiting being intercepted by other obstacle forward or diffuse and deposite on the obstacle, growing into large water drops. The other part of the fog flow that falls to the middle part of the obstacle's projection plane will advance and collide with the obstacle, and the tiny water drops carried by it will be interpected directly. Namely, tiny water drops carried by the fog flow progress along the flow to a large extent although there might be some drops that do not follow the flow due to their larger inertia. Therefore, the flow field, or the flow stream in visual representation, around a fog collector is crucial to the ultimate fog collection efficiency. Furthermore, the flow steam can be affected by many factors. Take a mesh-based fog collector as an example, the flow steam can vary dramatically because of difference in diameter and shape of the mesh fibers,[19] shading coefficient of the mesh[20,21] and most importantly, the microstructures of the fibers, which might induce tuberlance of the flow stream and favor of fog collection.[18,22]

In terms of the fog collection in our case, as can be seen from **Figure 4**, the fog flow streams differ from each other considerably on different structured surfaces. Figure 4A–C depicits a wide range of flow stream around surface with hexagonally arranged cones, surface with tetragonally arranged cones and the surface with microscale smoothness, respecively. Figure 4B–D are the corresponding local amplification. On a surface with hexagonally arranged cones, the staggered arrangment of cones induces that each cone is wholly wrapped by the flow stream (Figure 4A,C). So tiny water drops can not only deposit on the windward side but also on the leewind side of the cones. This enlarged depositon area contributes to the higher fog collection efficiency. Comparatively, the fog flow on the surface with tertagonally arranged cones can only reach the windside of the cones, leaving the leewind side vacuum of fog flow (Figure 4B,D). Tiny water drops deposit mostly on the windside, fewer on the side and nearly none on the leeside of the cones. With regards to the smooth surface, the solid surface is equal to the mesh with a shading coaefficient one.[23] In this situation, the fog flow carring tiny water drops will pass around due to the high resistance to flow through it (Figure 4C,E).[20] Therefore, the little portion of fog flow sweeping across the top

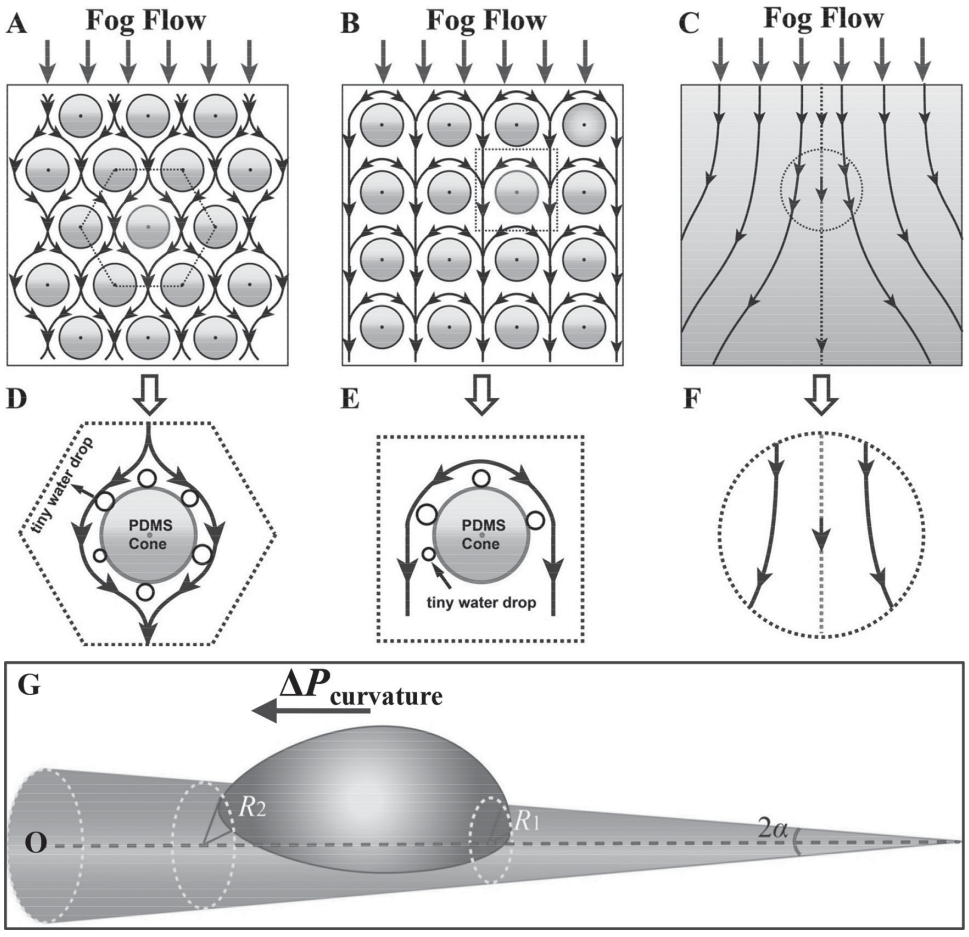

Figure 4. Mechanism of the different fog collection efficiency on different structured surfaces. A–C) different streamlines of fog flow around surfaces with hexagonally arranged cones, tetragonally arranged cones and solid surface with microscale smoothness. D–F) Magnified details of fog flow around each cone corresponding to (A–C). D) Cones are entirely wrapped by the fog and tiny drops can deposit on both the windward and leeward part of the cone. E) Front of the cone is wrapped leaving rear of it "vacuum of fog". Tiny water drops deposit on the windward of the cone but few on the leeward. F) Fog flow bears larger resistance to pass through the solid surface and most of it flows around the side of the surface with a little portion sweeping across the top surface, resulting in fewer drops being deposited. G) Water drops on the cone move directionally towards the region with larger curvature radius due to gradient of Laplace pressure $\Delta P_{curvature}$.

surface leads to few water drops intercepted. It is also pointed out that difference of the total surface area arising from the different structures of these three kinds of surfaces contributes little to the overall discrepancy of the fog collection efficiency (Supporting Information Figure S8).

2.3.2. Directional Movement of Water Drops on Cones

In addition to the distinct fog flow field around cone-structured surfaces and the smooth surface, directional movement of water drops on these surfaces heavily affects their fog collection efficiencey. Specifically, water drops on a cone-structured object feel different Laplace pressure in the two opposite sides. The side on the region with larger curvature radius senses smaller Laplace pressure and the side on the region with smaller curvature radius senses larger Laplace pressure.[11] This difference induces a gradient of Laplace pressure $\Delta P_{curvature}$ propeling water drops move directionally towards region with larger curvature radius (Figure 4F).

$$\Delta P_{curvature} = -\int_{R_1}^{R_2} \frac{2\gamma}{(R+R_0)^2} \sin\alpha \, dz$$

where, γ is the surface tention of water; R is the local radius of the cone (R_1 and R_2 are the local radii of the cone at two opposite sides of the water drop, R_0 is radius of the water drop),α is the half-apex angle of the cone and dz is the integral variable of the cone. When water drops on the cones move away, the original deposition sites are released and the continuous fog collection can be achieved. Unlike the directional movement on cones, water drops on the smooth surface increase their volume without regular change of mass center due to non-existence of gradient. The resulting absence of quick regeneration of the deposition sites is adverse to the efficient fog collection. Therefore, the fog collection efficiency of a smooth surface is accordingly the lowest.

3. Conclusion

In conclusion, we find that in addition to the clusters of spines on the cactus stem, the intersite is densely covered with cones, which are efficient in fog collection. Inspired by these cones, we designed and fabricated artificial PDMS cone arrays with different arrangements using a simple method combining mechanical perforating and template replica technology. The as prepared cone-structured surface with hexagonally arranged cones shows obvious advantages compared to the surface with tetragonally arranged cones and a smooth surface. The underlying mechanism has two aspects: first, the more tuberlent and complicated flow field around the stagged cones increases the effctive depositon area, facilitating more tiny water drops' deposition and the ultimate fog collection; second, the directional transport of water drops collected on the cone-structured surface benefits the quick rebirth of the deposition sites, and further favors efficient fog collection. This bioinspired design opens up a new avenue to collect water efficiently and may be potentially useful for relieving the water crisis in arid regions. Additionally, the investigation of the different collection efficiencies of structured surfaces may also provide insight that is useful for dust filtering[10,19] and smog removal,[24] which are attracting increasing attention worldwide.

4. Experimental Section

Preparation of Surfaces with PDMS Cone Arrays: To fabricate the cone arrays with desired arrangement, a stainless steel needle fixing onto a programmable jet dispensing system was firstly exploited to punch regular holes on a commercial low-density polyethylene (LDPE) sheet. Then, PDMS (Sylgard 184, Dow Coring) was used to replicate the structures. After peeling off the LDPE template, a PDMS surface with designed arrangement of cones can be obtained. The as-prepared PDMS cone arrays were used without further treatment.

Fog Collection Details on Different Kinds of Surfaces: The natural cactus stem without clusters of spines, the bioinspired surfaces with cone arrays and the artificial smooth PDMS surface were sequentially placed under a stereomicroscope (Zeiss, Discovery V 8.0, Germany). A sustained fog flow with a velocity of about 125 cm s^{-1}, generated by an ultrasonic humidifier (YC-E350, China), was set to blow the cones and the smooth surface with a tilt angle of δ to the tangent direction of the substrate at the room temperature (Supporting Information Scheme S1). The fog collection processes were recorded by a CCD component matched with the microscope. The top-view and side-view details of the fog collection can be obtained by simply tuning the placement directions of the surfaces for fog collection.

Measurement of the Fog Collection Ability: To assess the fog collection ability of these four kinds of surfaces, the mass change of these surfaces (1 cm by 1 cm) under fog flow in a period of time was investigated. In detail, the four surfaces were placed in sequence on a slender bracket (with height and width of about 10 cm and 1 cm) fixed on the table of microelectronic balance (Mettler Toledo, XS205DU, Switzerland) to reduce influence from the table of microelectronic balance. The fog collection surface is set to have a titled angle θ to the horizontal plane for facilitating water drain. A fog flow similar to the above was introduced to blow these surfaces. A digital camera (Canon EOS 60D, Japan) was used to record the balance reading change with prolonged time. The fog collection on polypropylene mesh, kept the same placement of the mesh as above, but the fog flow was changed to be perpendicular to the surface. The mass change of it was also recorded using the highly sensitive balance system.

Characteristic of Surface Structures: The optical microscopic images were obtained using a digital camera (Canon EOS 60D, Japan). The SEM images were obtained using a field-emission scanning electron microscopy (Hitachi S4800, Japan).

Supporting Information

Supporting Information is available from the Wiley Online Library or from the author.

Acknowledgements

X.Y. and S.Y. contributed equally to this work. This work was supported by National Research Fund for Fundamental Key Projects (2013CB933000 and 2012CB934100), National Natural Science Foundation (21121001, 91127025), the Key Research Program of the Chinese Academy of Sciences (KJZD-EW-M01) and the 111 project (B14009).

Received: July 6, 2014
Published online: September 1, 2014

[1] a) E. S. Shanyengana, J. R. Henschel, M. K. Seely, R. D. Sanderson, *Atmos. Res.* **2002**, *64*, 251; b) J. Olivier, C. J. de Rautenbach, *Atmos. Res.* **2002**, *64*, 227.
[2] H. G. Andrews, E. A. Eccles, W. C. E. Schofield, J. P. S. Badyal, *Langmuir* **2011**, *27*, 3798.
[3] A. R. Parker, C. R. Lawrence, *Nature* **2001**, *414*, 33.
[4] A. Roth-Nebelsick, M. Ebner, T. Miranda, V. Gottschalk, D. Voigt, S. Gorb, T. Stegmaier, J. Sarsour, M. Linke, W. Konrad, *J. R. Soc. Interface* **2012**.
[5] a) L. Zhai, M. C. Berg, F. Ç. Cebeci, Y. Kim, J. M. Milwid, M. F. Rubner, R. E. Cohen, *Nano Lett.* **2006**, *6*, 1213; b) R. P. Garrod, L. G. Harris, W. C. E. Schofield, J. McGettrick, L. J. Ward, D. O. H. Teare, J. P. S. Badyal, *Langmuir* **2007**, *23*, 689; c) S. C. Thickett, C. Neto, A. T. Harris, *Adv. Mater.* **2011**, *23*, 3718; d) B. White, A. Sarkar, A.-M. Kietzig, *Appl. Surf. Sci.* **2013**, *284*, 826.
[6] H. Yang, H. Zhu, M. M. R. M. Hendrix, N. J. H. G. M. Lousberg, G. de With, A. C. C. Esteves, J. H. Xin, *Adv. Mater.* **2013**, *25*, 1150.
[7] B. S. Lalia, S. Anand, K. K. Varanasi, R. Hashaikeh, *Langmuir* **2013**, *29*, 13081.
[8] a) J. Ju, H. Bai, Y. Zheng, T. Zhao, R. Fang, L. Jiang, *Nat. Commun.* **2012**, *3*, 1247; b) J. Ju, Y. Zheng, L. Jiang, *Acc. Chem. Res.* DOI: 10.1021/ar5000693.
[9] Y. Zheng, H. Bai, Z. Huang, X. Tian, F.-Q. Nie, Y. Zhao, J. Zhai, L. Jiang, *Nature* **2010**, *463*, 640.
[10] H. Bai, J. Ju, Y. Zheng, L. Jiang, *Adv. Mater.* **2012**, *24*, 2786.
[11] É. Lorenceau, D. Quéré, *J. Fluid Mech.* **2004**, *510*, 29.
[12] J. Ju, K. Xiao, X. Yao, H. Bai, L. Jiang, *Adv. Mater.* **2013**, *25*, 5937.
[13] K. Li, J. Ju, Z. Xue, J. Ma, L. Feng, S. Gao, L. Jiang, *Nat. Commun.* **2013**, *4*, 2276.
[14] H. Bai, X. Tian, Y. Zheng, J. Ju, Y. Zhao, L. Jiang, *Adv. Mater.* **2010**, *22*, 5521.
[15] a) S. Daniel, M. K. Chaudhury, J. C. Chen, *Science* **2001**, *291*, 633; b) J. B. Boreyko, C.-H. Chen, *Phys. Rev. Lett.* **2009**, *103*, 184501.
[16] R. Chen, X. Zhang, Z. Su, R. Gong, X. Ge, H. Zhang, C. Wang, *J. Phys. Chem. C* **2009**, *113*, 8350.
[17] M. Cao, J. Ju, K. Li, K. Liu, L. Jiang, *Adv. Funct. Mater.* **2014**, *24*, 3235.
[18] C. Martorell, E. Ezcurra, *Oecologia* **2007**, *151*, 561.
[19] S. A. Hosseini, H. V. Tafreshi, *Powder Technol.* **2011**, 425–431.
[20] K.-C. Park, S. S. Chhatre, S. Srinivasan, R. E. Cohen, G. H. McKinley, *Langmuir* **2013**.
[21] J. d. D. Rivera, *Atmos. Res.* **2011**, *102*, 335.
[22] S. Vogel, U. Mueller-Doblies, *Flora* **2011**, *206*, 3.
[23] R. S. Schemenauer, P. Cereceda, *J. Appl. Meteorol.* **1994**, *33*, 1313.
[24] L. Caceres, J. Delatorre, B. Gomez-Silva, V. Rodriguez, C. P. McKay, *Atmos. Res.* **2004**, *71*, 127.